

# TWO-LOOP SELF-ENERGY CORRECTIONS TO ONE-PHOTON RECOMBINATION PROCESS IN HYDROGEN ATOM

*P. Kvasov*<sup>a</sup>, *A. Bobylev*<sup>a,b</sup>, *J. J. Lopez-Rodriguez*<sup>a</sup>, *D. Solovyev*<sup>a,b</sup>, *E. Solovyeva*<sup>c</sup>,  
*T. Zaliatiutdinov*<sup>a,b\*</sup>

<sup>a</sup> *Department of Physics, St. Petersburg State University  
198504, St. Petersburg, Russia*

<sup>b</sup> *Petersburg Nuclear Physics Institute  
188300, Gatchina, St. Petersburg, Russia*

<sup>c</sup> *Chemistry Institute, St. Petersburg State University  
198504, Peterhof, St. Petersburg, Russia*

Received October 12, 2025,  
revised version November 14, 2025  
Accepted for publication November 14, 2025

In the framework of relativistic quantum electrodynamics, two-loop self-energy corrections to the cross section of one-photon recombination are investigated for bound states. Using the hydrogen atom as an example, it is demonstrated that the derived analytical expression is free from singular contributions, in contrast to the expression for the cross section of two-photon recombination, which inevitably contains inseparable resonant contributions corresponding to cascade one-photon transitions. Utilizing the obtained expression, numerical calculations of the two-photon part of the radiative correction to the spontaneous one-photon recombination coefficient are performed under the assumption of a Maxwellian distribution of free electrons. By employing a three-level recombination model for the primordial hydrogen plasma in the early Universe, it is demonstrated that the derived corrections to the ionization degree of primordial plasma approach the level of numerical precision typically required in theoretical recombination models, but remain below the current experimental sensitivity.

**Keywords:** quantum electrodynamics of bound states, two-loop corrections, electron self-energy, atomic recombination, Hydrogen atom.

DOI: 10.31857/S3034641X26010022

## 1. INTRODUCTION

In recent years, precise cosmological observations have placed increasingly stringent demands on theoretical models of the early Universe [1, 2]. Among these, the process of hydrogen recombination in the primordial plasma plays a central role in determining the ionization history and, consequently, parameters of cosmological models. Following the seminal work of Peebles and Zeldovich [3, 4], significant progress was achieved through studies by Seager, Sasselov, and Scott, who developed a comprehensive model of recombination kinetics [5, 6]. These works established a framework for sys-

tematically studying subtle physical effects influencing the recombination history and opened avenues for exploring new physics beyond the Standard Model [7, 8].

The increasing experimental precision in measuring the temperature and polarization anisotropies of the Cosmic Microwave Background (CMB) over the past 20 years has necessitated continuous refinement of theoretical models, including high-accuracy treatments of various atomic processes and radiative transfer [9, 10]. Current observational requirements demand a relative theoretical accuracy of at least 0.1% for recombination models. It is generally accepted that effects contributing to the formation of CMB at the 0.001% level, including exotic scenarios such as dark matter annihilation, have already been identified and incorporated into modern recombination codes [11, 12]. Despite this, the discrepancies between the cosmological parameters

\* E-mail: t.zaliatiutdinov@spbu.ru

derived from various astrophysical observations suggest that the models employed to explain the recombination epoch of the Universe need to be improved [1]. In particular, reassessing these models should include careful calculations of radiation–matter interactions during hydrogen recombination [9].

To meet these demands, it is essential to systematically account for all physical effects contributing to the ionization and recombination rates at a level beyond current approximations. Among these contributions, quantum electrodynamic (QED) radiative corrections reflect fundamental effects from the relativistic interactions of electrons, protons, and photons. While typically small, these corrections may play a non-negligible role in achieving the required theoretical precision and could potentially affect the predicted recombination history of the Universe.

Earlier, we demonstrated that certain quantum electrodynamical (QED) effects, particularly those arising from the finite lifetime of excited atomic states, induce corrections to the bound-bound transition rates [13–15] and the cross sections for one-photon recombination [16]. These corrections were found to influence the degree of ionization at a level comparable to current experimental and theoretical accuracies.

In the present work, we consider the two-photon radiative correction to the one-photon recombination process. Particular attention is paid to the nonresonant contributions to the two-photon process, as they directly contribute to the decoupling of radiation. The calculation of two-photon corrections is carried out based on the methodology developed in [13, 17], see originally [18–20].

This paper is organized as follows. In Section 3, we derive the cross section for one-photon recombination of the hydrogen atom by evaluating the imaginary part of the one-loop self-energy operator, averaged over the continuum electron wave functions in the nuclear Coulomb field. Section 4 focuses on the derivation of cross sections for the two-photon recombination process within the framework of the Line Profile Approach (LPA) [21]. Section 5 then explores the two-photon contribution to the two-loop self-energy operator, again averaged over continuum states. In Section 6, the numerical approaches are briefly discussed. Section 7 considers the impact of the two-photon contribution from the two-loop self-energy radiative correction to the one-photon recombination coefficient on the ionization fraction of primordial hydrogen plasma. Throughout this paper, we employ relativistic units where  $\hbar = c = m_e = 1$  and charge units  $\alpha = e^2$ , where  $\alpha$  is the fine structure constant.

## 2. THE $n_\gamma$ -LOOP APPROACH ( $n_\gamma$ LA): FUNDAMENTAL CONCEPTS

In the context of atomic and molecular spectroscopy, one of the key parameters characterizing the system being studied is the natural width of the excited state (which is zero for the ground state). It is well known that the total natural width,  $\Gamma_a$ , of a bound atomic state  $a$  can be determined as the sum of all spontaneous partial transition rates to lower-lying atomic states  $b$ :

$$\Gamma_a = \sum_{E_b \leq E_a} W_{ab}, \tag{1}$$

where  $W_{ab}$  is the partial transition probability for the process  $a \rightarrow b$ ,  $E_a$  and  $E_b$  represent the corresponding energies of the levels  $a$  and  $b$ , respectively.

According to the basic principles of quantum theory, the partial quantities include the sum of all one-, two-, three-, etc. transition rates allowed by the selection rules [22]:

$$W_{ab} = W_{ab}^{(1\gamma)} + W_{ab}^{(2\gamma)} + W_{ab}^{(3\gamma)} + \dots \tag{2}$$

Possessing an additional smallness in the fine structure constant  $\alpha$ , each subsequent  $n_\gamma$  emission probability, which enters expression Eq. (2), can be considered within the context of perturbation theory, for example, within the framework of Feynman diagram techniques and the S-matrix formalism. The application of the latter is a separate area of theoretical research, covering not only the determination of the natural level width as the combination of Eqs. (1), (2) but also the calculation of various corrections within the framework of QED theory, see, e. g., [23, 24].

An alternative approach is also widely recognized, which focuses not on the photon scattering processes (reduced to the radiation process [15]), but the self-energy correction of a bound electron using QED methods. Within the framework of relativistic quantum electrodynamic theory, the level width Eq. (1) can be obtained by considering the imaginary part of the one-loop ( $n_\gamma = 1$ ) self-energy correction  $\Delta E_a^{\text{SE}}$  [25, 26]:

$$\Gamma_a = -2\text{Im} \Delta E_a^{\text{SE}}. \tag{3}$$

This correction is represented by the Feynman diagram shown in Fig. 1.

Without addressing the issues of calculating the real part of this correction (contribution to the Lamb shift of the atomic level [27]), the imaginary part is calculated quite simply without requiring the use of QED

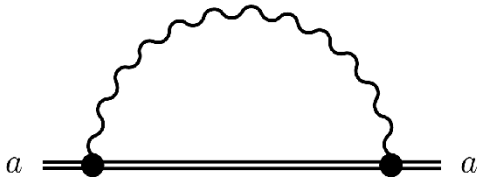


**Fig. 1.** Feynman diagram representing the one-loop self-energy correction for a bound electron in the state  $a$ . The double line represents the electron propagator in the Coulomb field of the nucleus (Furry picture), while the wavy line indicates the virtual photon loop

renormalization theory. The detailed calculations of the one-loop self-energy correction can be found in [25], where a closed relativistic expression for  $\Gamma_a$  was provided. Within the nonrelativistic limit the found expression coincides with commonly accepted Eq. (1).

In general, the proof of expression (3) is limited to the one-loop case, i.e. to the partial transition rates accounting for only one-photon decay processes,  $W_{ab} = W_{ab}^{(1\gamma)}$ . Using the  $n_\gamma$ -loop approach ( $n_\gamma$ LA) to determine the natural width in the next order of perturbation theory ( $n_\gamma$ -photon emission process) requires a separate careful consideration. The corresponding ( $n_\gamma = 2$ )-loop diagrams are depicted in Figs. 2. It is expected that going beyond the one-loop approximation leads to multiphoton contributions to the natural level width (see Eq. 2). However, the definition of a multi-photon ( $n_\gamma \geq 2$ ) natural level width within the framework of  $n_\gamma$ LA has encountered a number of conceptual difficulties.

Regardless, the initial source of all complications is the two-photon decay of highly excited states. In such transitions, the dominant decay channel turns out to be a one-photon transition to an intermediate (resonant) state, which also decays via a one-photon process to the ground energy level. This two-photon decay defines a two-photon cascade of radiation, the probability of which is influenced by a one-photon partial probability. Thus, in the  $n_\gamma$ -decay probability of a highly excited state, there is always a one-photon quantity present, which is already taken into account according to Eq. (2). Such a recursive procedure should be avoided. It should be noted that this pattern occurs regardless of whether the process of  $n_\gamma$ -radiation or  $n_\gamma$ LA is considered [28].

To address this issue, the following query emerged (also quite well-known, see [29] and references therein).

The recursive accounting of one-photon contributions can be avoided by separating cascade radiation from the nonresonant («pure») two-photon decay process. It turns out that cascade radiation is inseparable from a small nonresonant contribution due to the interference between them. The interference may be of the same order as the «pure» radiation [13, 17, 28]. The problem of correctly accounting for two-photon decays for bound-bound transitions and its application to evaluation of the recombination kinetics of primordial hydrogen plasma in the early universe has been intensively discussed in the last decades. Different approaches were employed, each with its own drawbacks [30–35]. To avoid redundancy, we do not explore into the specifics of the approximations used in the literature for estimating two-photon widths. Instead, we direct the reader to the review [15]. A comprehensive analysis of the complex problem of distinguishing between one-photon (cascade) emission and the simultaneous two-photon component has also been performed in [36].

However, it can be shown that the imaginary part of the two-loop self-energy diagrams in Fig. 2 entails the appearance of two-photon widths [18–20]. This scenario is rather unique and pertains to the absence of cascade radiation in the two-photon decay process, see the discussion in [13, 17, 28, 36]. The distinct advantage of the two-loop formalism is that the two-photon width does not contain cascade processes and turns out to be regular (the presence or absence of a cascade process in two-photon decay is irrelevant) [18–20]. This finding, based on the «alternative approach» outlined in [18–20], appears to be particularly relevant for research of the radiation transfer [5, 6]. However, as was shown in [13], the value calculated in this way can be negative and, therefore, the corresponding quantity should be interpreted as a radiative correction to the one-photon transition rate. Being of the same order as the well-known probability of two-photon  $2s - 1s$  decay in a hydrogen atom, this correction turns out to be significant for studies of CMB formation processes, see, e. g., [30, 34].

Based on the one- and two-loop approach, in the following sections we calculate the correction to the cross section of the one-photon recombination process of the hydrogen atom. Since only bound-bound transitions have been discussed above, we find it appropriate to give a brief summary of the  $n_\gamma$ LA method for the case of free-bound transitions; for details and relevant calculations, see [16]. Then, the combination of the «alternative approach» [18–20] and  $n_\gamma$ LA obviously reduces to a two-photon process.

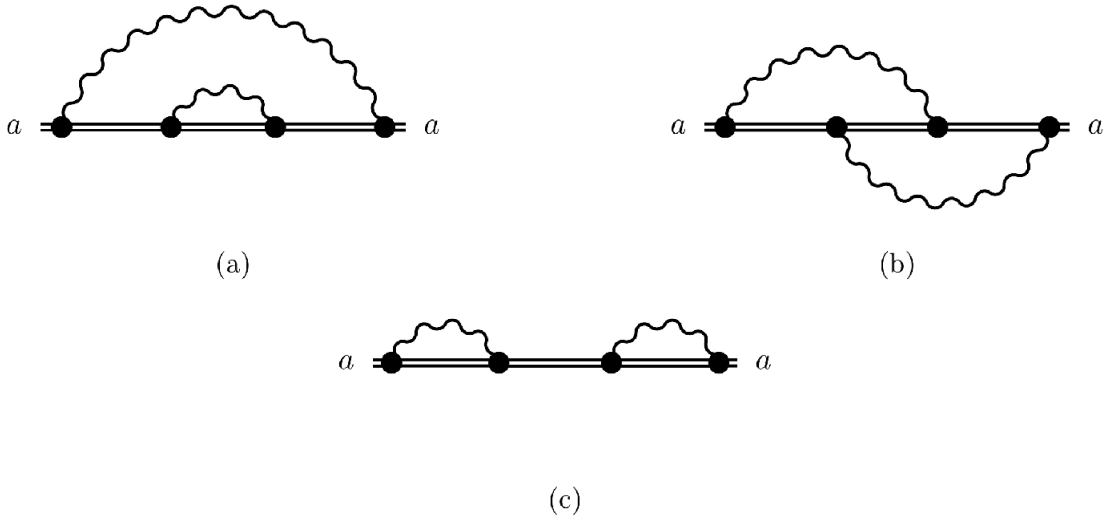


**Fig. 2.** Feynman diagrams for two-loop self-energy corrections for the bound electron in the state  $a$ : (a) loop inside loop, (b) crossed loops, and (c) loop-after-loop contributions. The imaginary contributions from the poles of intermediate electron propagators can be given by «cuts», see below. All notations are the same as in Fig. 1

**3. ONE-PHOTON RECOMBINATION CROSS SECTION: ONE-LOOP APPROACH**

Recently, the  $n_\gamma$ LA was extended to free-bound transitions in [16]. In particular, it was shown that the imaginary part of the self-energy operator averaged over the states of free-electron in the Coulomb field of nuclei results in the closed expression for the total one-photon recombination cross section:

$$\sigma_{\text{rec}}^{\text{tot}} = \sum_n \sigma_{\varepsilon n}^{(1\gamma)}. \tag{4}$$

Here summation over  $n$  implies sum over the discrete bound states,  $\sigma_{\varepsilon n}^{(1\gamma)}$  is the partial one-photon recombination cross section of an electron with energy  $\varepsilon$  to the bound state  $n$ .

Following [16], we briefly outline the derivation of the one-photon recombination cross section using the one-loop approach. According to the Feynman rules in the Furry picture, the general off-diagonal S-matrix element, corresponding to Fig. 1 with the choice  $a = \varepsilon$ , is expressed as follows:

$$\begin{aligned} \langle a' | \widehat{S}^{(2)} | a \rangle &= \\ &= (-ie)^2 \int d^4x_1 d^4x_2 \bar{\psi}_{a'}(x_1) \gamma^\mu S(x_1, x_2) \gamma^\nu \times \\ &\quad \times D_{\mu\nu}(x_1, x_2) \psi_a(x_2). \end{aligned} \tag{5}$$

The Dirac matrices are denoted as  $\gamma_\mu$ , where indexes take the values  $\mu, \nu = (0, 1, 2, 3)$ ,  $\psi_a(x) = \psi_a(\mathbf{r})e^{-i\varepsilon_a t}$  is the one-electron Dirac wave function ( $\varepsilon_a$  is the corresponding energy of the state  $a$ ),  $\bar{\psi}_a$  is the Dirac conjugated wave function. Integration takes place along 4-dimensional coordinates  $x_i \equiv \{t_i, \mathbf{r}_i\}$ ,  $t_i$  is the time coordinate and  $\mathbf{r}_i$  is the spatial position vector of a bound electron.

In Eq. (5)  $D_{\mu_1\mu_2}(x_1, x_2)$  denotes the photon propagator

$$D_{\mu\nu}(x_1, x_2) = \frac{g_{\mu\nu}}{2\pi i r_{12}} \int_{-\infty}^{\infty} e^{-i\omega(t_1-t_2)+i|\omega|r_{12}} d\omega, \tag{6}$$

where  $g_{\mu\nu}$  is a metric tensor (hereafter we use the Euclidean metric) and  $r_{12} \equiv |\mathbf{r}_1 - \mathbf{r}_2|$ . The elec-

tron propagator  $S(x_1, x_2)$  can be set as an eigen-mode decomposition [27]

$$S(x_1, x_2) = \frac{i}{2\pi} \int_{-\infty}^{\infty} d\Omega e^{-i\Omega(t_1-t_2)} \sum_n \frac{\bar{\psi}_n(\mathbf{r}_1)\psi_n(\mathbf{r}_2)}{\Omega - \mathcal{E}_n(1-i0)}. \quad (7)$$

The sum over  $n$  in Eq. (7) runs over the entire Dirac spectrum.

For the one-loop irreducible Feynman diagram the corresponding energy shift can be found as diagonal matrix element ( $a' = a$ ):

$$\Delta E_a^{\text{SE}} = \langle a | \hat{U}^{(2)} | a \rangle, \quad (8)$$

where  $U^{(2)}$  is the amplitude of the process defined by the relation:

$$\langle a' | \hat{S}^{(2)} | a \rangle = -2\pi i \delta(\mathcal{E}_{a'} - \mathcal{E}_a) \langle a' | \hat{U}^{(2)} | a \rangle. \quad (9)$$

By integrating over the time and frequency variables in the expression (5) and taking into account that the state  $a$  belongs to the continuum spectrum  $a \equiv \varepsilon$ , we obtain

$$\Delta E_\varepsilon^{\text{SE}} = \frac{e^2}{2\pi i} \sum_n \left( \frac{1 - \alpha_1 \alpha_2}{r_{12}} I_{\varepsilon n}(r_{12}) \right)_{\varepsilon n n \varepsilon}. \quad (10)$$

The matrix element  $(\hat{A}^{(12)})_{abcd}$  should be understood as  $\langle \bar{\psi}_a(1) \bar{\psi}_b(2) | \hat{A}^{(12)} | \psi_c(1) \psi_d(2) \rangle$  and

$$I_{\varepsilon n}(r_{12}) = \int_{-\infty}^{\infty} d\omega \frac{e^{i|\omega|r_{12}}}{\mathcal{E}_n(1-i0) - \varepsilon + \omega}. \quad (11)$$

To derive the recombination cross section  $\sigma_{\text{rec}}$  from one-loop self-energy correction in [16] it was suggested to consider the imaginary part of  $\Delta E_\varepsilon$ , i.e., the real part of the integral  $I_{\varepsilon n}(r_{12})$ . Accordingly, this integral can be presented in the form

$$I_{\varepsilon n}(r_{12}) = \int_{-\infty}^{\infty} \frac{e^{i\omega r_{12}}}{\mathcal{E}_n - \varepsilon + \omega \mp i0} d\omega - 2i \int_{-\infty}^0 \frac{\sin \omega r_{12}}{\mathcal{E}_n - \varepsilon + \omega \mp i0} d\omega. \quad (12)$$

In the second integral in Eq. (12), we can omit  $\mp i0$  from the denominator, since this denominator does not have zeros within the interval  $(-\infty, 0]$ . Thus, the second term on the right-hand side of Eq. (12) is pure imaginary, and we omit its consideration in further. Combined with the pre-factor  $i$  in Eq. (10), a purely real

quantity arises, which is irrelevant for the continuum energy spectrum of the electron.

The sign  $\mp$  in the denominator of the first integral corresponds to  $E_n < 0$ ,  $E_n > 0$  (negative and positive Dirac energy spectra). Evaluating this integral in the complex plane we close the contour of integration in the upper half-plane since in this half-plane the integral vanishes along the half-circle with infinitely large radius. The existence of the pole inside this contour depends on the sign of  $E_n$ ; the pole exists when  $E_n > 0$ . Evaluation of residue in this pole gives

$$\text{Re}[I_{\varepsilon n}(r_{12})] = 2\pi \sin((\varepsilon - \mathcal{E}_n)r_{12}), \quad (13)$$

and finally we obtain the closed expression for  $\Gamma_\varepsilon^{(1\gamma)}$ :

$$\Gamma_\varepsilon^{(1\gamma)} = -2 \text{Im} \Delta E_\varepsilon = 2e^2 \sum_{\varepsilon_n > 0} \left( \frac{1 - \alpha_1 \alpha_2}{r_{12}} \sin((\varepsilon - \mathcal{E}_n)r_{12}) \right)_{\varepsilon n n \varepsilon}. \quad (14)$$

Here, the summation is carried out over a discrete set of states from the positive Dirac energy spectrum.

The expression (3) is similar to the total one-photon radiative natural width [25,26]. The quantity  $\Gamma_\varepsilon^{(1\gamma)}$  can be associated with one-photon photo-recombination of an one-electron atom in the following way. Going to the non-relativistic limit we find:

$$\Gamma_\varepsilon^{(1\gamma)} = \frac{4}{3} e^2 \sum_n (\varepsilon - \mathcal{E}_n) |\langle \varepsilon | \mathbf{p} | n \rangle|^2. \quad (15)$$

To obtain the cross section we should divide Eq. (39) by the flux of incident electrons  $j = nv$  ( $v$  is the velocity of particle,  $n$  is the number of electrons) with  $n = 1$  [16]:

$$\sigma_{\text{rec}}^{(1\gamma)} = \frac{\Gamma_\varepsilon^{(1\gamma)}}{j}. \quad (16)$$

The wave function for the continuum state with energy  $\varepsilon = p^2/2$ , can be expressed as [25]

$$\psi_p = \frac{1}{2p} \sum_{l=0}^{\infty} i^l (2l+1) e^{i\delta_l} R_{pl}(r) P_l(\cos \theta), \quad (17)$$

where  $R_{pl}(r)$  is the radial part of the hydrogen wave function,  $\theta$  is the angle between vectors  $\mathbf{r}$  and  $\mathbf{p}$ , and the phase factor  $\delta_l$  can be omitted as immaterial for our purposes. It is important to note that the cross section for one-photon recombination, as given by Eq. (16) and derived using the loop approach, aligns with the S-matrix approach for the one-photon emission process, describing the free-bound electron transition in the field of nucleus [21].

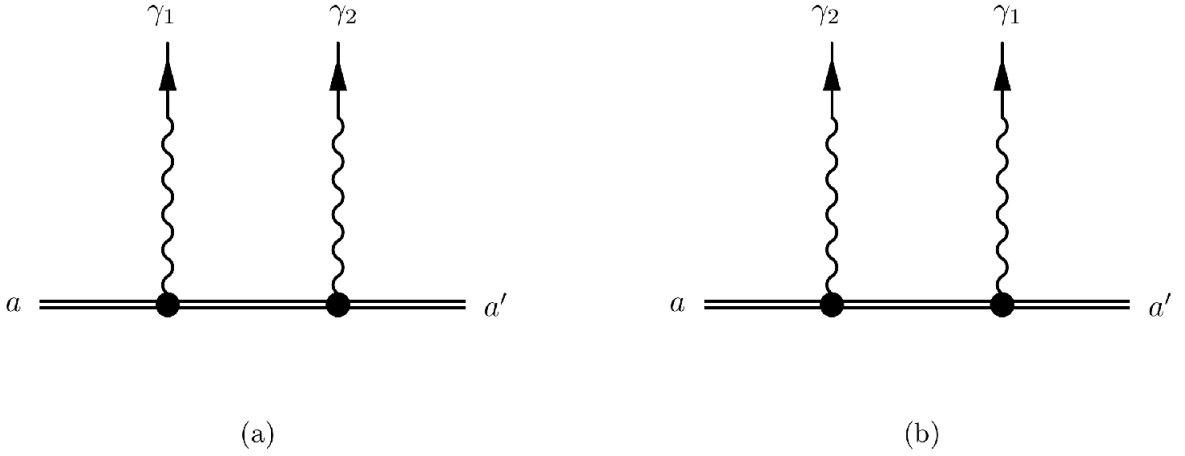


**Fig. 3.** Feynman diagrams contributing to the cross section of two-photon recombination. The wavy lines with arrows indicate the emitted photons, which are numbered as  $\gamma_1$  and  $\gamma_2$ . The two graphs (a) and (b) arise due to the permutation symmetry of the photons. The other notations are the same as in Fig. 1

**4. TWO-PHOTON RECOMBINATION CROSS SECTION: EMISSION PROCESS**

Before proceeding to the main derivation of the two-photon part of the two-loop self-energy correction to the cross section of one-photon recombination for subsequent comparative analysis, it is necessary to derive an analytical expression for the cross section of electron recombination with the emission of two photons. The required expression can be obtained in complete analogy with the derivation of the multi-photon probability for bound-bound transitions. The Feynman diagrams showing the two-photon emission process are illustrated in Fig. 3.

The transition probability amplitude for the two-photon decay  $a \rightarrow a' + 2\gamma$  (here the initial state  $a = \varepsilon$  represents an electron with momentum  $p$  and energy  $\varepsilon = \frac{p^2}{2m}$  in the continuum spectrum in the Coulomb field of the nucleus) is given by the second-order S-matrix elements for the diagrams shown in Fig. 3 a:

$$\begin{aligned} \langle a' | \hat{S}^{(2)} | a \rangle &= \\ &= (-ie)^2 \int d^4x_1 d^4x_2 \times \\ &\times \bar{\psi}_{a'}(x_1) \gamma^{\mu_1} A_{\mu_1}^*(x_1) S(x_1, x_2) \gamma^{\mu_2} A_{\mu_2}^*(x_2) \psi_a(x_2). \end{aligned} \tag{18}$$

Here all notations are the same as for Eq. (5). The photon wave-function in the coordinate space representation is

$$A_\mu(x) = \sqrt{\frac{2\pi}{\omega}} e_\mu^\lambda e^{i\omega t - i\mathbf{k}\mathbf{r}}, \tag{19}$$

where four-polarization vector is given by  $e_\mu^\lambda$  ( $\lambda = 0, \pm 1$ ), the wave-vector is denoted by  $\mathbf{k}$  and with the corresponding frequency  $\omega = |\mathbf{k}|$  [27]. The differential transition rate is determined using the ratio (9) and is given by

$$\begin{aligned} dW_{a'a}^{(2\gamma)}(\mathbf{k}, \mathbf{e}) &= 2\pi \left| U_{a'a}^{(2)} \right|^2 \delta(\omega + \omega' - \mathcal{E}_a + \mathcal{E}_{a'}) \times \\ &\times \frac{d\mathbf{k}}{(2\pi)^3} \frac{d\mathbf{k}'}{(2\pi)^3}. \end{aligned} \tag{20}$$

By performing integration over time variables and frequency  $\Omega$  in Eq. (7), the expression (18), combined with the exchange contribution, see Fig. 3 b, results in two-photon emission amplitude:

$$\begin{aligned} U_{a'a}^{(2)} &= \frac{2\pi e^2}{\sqrt{\omega\omega'}} \left[ \sum_n \frac{\langle a' | \boldsymbol{\alpha} \mathbf{A}_{\mathbf{k}\lambda}^* | n \rangle \langle n | \boldsymbol{\alpha} \mathbf{A}_{\mathbf{k}'\lambda'}^* | a \rangle}{\mathcal{E}_n - \mathcal{E}_a + \omega'} + \right. \\ &\left. + \sum_n \frac{\langle a' | \boldsymbol{\alpha} \mathbf{A}_{\mathbf{k}'\lambda'}^* | n \rangle \langle n | \boldsymbol{\alpha} \mathbf{A}_{\mathbf{k}\lambda}^* | a \rangle}{\mathcal{E}_n - \mathcal{E}_a + \omega} \right], \end{aligned} \tag{21}$$

where  $\mathbf{A}_{\mathbf{k}\lambda} \equiv \mathbf{e}_{\mathbf{k}\lambda} e^{i\mathbf{k}\mathbf{r}}$  [15]. Going to the nonrelativistic limit,  $\mathbf{k}\mathbf{r} \ll 1$ , and the length-form of the matrix elements, see [25], we find

$$\begin{aligned} U_{a'a}^{(2)} &= 2\pi e^2 \sqrt{\omega\omega'} \left[ \sum_n \frac{\langle a' | \mathbf{r} \mathbf{e}_{\mathbf{k}\lambda}^* | n \rangle \langle n | \mathbf{r} \mathbf{e}_{\mathbf{k}'\lambda'}^* | a \rangle}{E_n - E_a + \omega'} + \right. \\ &\left. + \sum_n \frac{\langle a' | \mathbf{r} \mathbf{e}_{\mathbf{k}'\lambda'}^* | n \rangle \langle n | \mathbf{r} \mathbf{e}_{\mathbf{k}\lambda}^* | a \rangle}{E_n - E_a + \omega} \right]. \end{aligned} \tag{22}$$

Here, the matrix elements are evaluated using Schrödinger wave functions, with  $E_n$  and  $E_a$  representing the non-relativistic energies.

Performing integration over the photon frequency  $\omega'$  (utilizing the  $\delta$ -function in Eq. (20)) and summation over the photon polarizations, the differential transition rate reduces to

$$dW_{a'a}^{(2\gamma)} = \frac{8e^4 \omega^3 (E_a - E_{a'} - \omega)^3}{9\pi (2l_a + 1)} \times \sum_{m_{a'} m_a} \left| \sum_n \left( \frac{\langle a' | \mathbf{r} | n \rangle \langle n | \mathbf{r} | a \rangle}{E_n - E_a + \omega} + \frac{\langle a' | \mathbf{r} | n \rangle \langle n | \mathbf{r} | a \rangle}{E_n - E_{a'} - \omega} \right) \right|^2 d\omega. \quad (23)$$

Then the total two-photon transition rate is

$$W_{a'a}^{(2\gamma)} = \frac{1}{2} \int_0^{E_a - E_{a'}} dW_{a'a}^{(2\gamma)}. \quad (24)$$

The total cross section for the recombination from a continuum state  $\varepsilon$  to a bound state  $a'$  is determined by the  $W_{a'a}^{(2\gamma)}$  in the way similar to the relation (16), i.e. by dividing the transition probability by the flux density of incident electron. Then,

$$\sigma_{a'}^{(2\gamma)} = \frac{W_{a'\varepsilon}^{(2\gamma)}}{j}. \quad (25)$$

The main difficulty in calculating expressions of the type (23) is to sum up the entire intermediate spectrum of  $n$ , including the continuum. There are various approaches to solving this problem. In particular, this can be achieved using either the Green's function method, see, e.g., [37–39], and references therein or by directly summing over the entire spectrum of states, employing explicit analytical expressions for the matrix elements [30]. In our work, we utilize the B-spline approach [40, 41], which is briefly discussed in section 6.

If there are intermediate states between states  $a$  and  $a'$ , the denominator of expression (23) can turn to zero, when the remaining frequency integral is taken Eq. (24). This situation corresponds to the cascade radiation, when two resonant photons are emitted. To eliminate the divergence in this expression, it is necessary to account for the radiative corrections to the energies in the denominator. Procedure of such regularization was proposed in [42], when an infinite series of successive one-loop self-energy corrections for a bound electron is taken into account (loop after loop) [15]. As a result, a natural width of levels arises in the resonance denominators, see also [21] for details.

In contrast to the works [13, 17], which considered two-photon transitions with cascades between bound states of the discrete spectrum, we are interested in the case when the initial state  $a$  belongs to the continuum energy spectrum of the electron in the Coulomb field of the nucleus. This leads to the emergence of an infinite number of intermediate resonances in the expression for the cross section, each of which should be regularized according to the procedure mentioned above. As a result, upon integration over all momenta of the incident electron, resonant contributions dominate the total cross section of two-photon recombination, with their magnitude comparable to that of the one-photon contribution. Due to the inseparability of nonresonant and cascade contributions caused by their interference, see [28, 43] and discussion in section 2, we encounter the same challenge as in bound-bound transitions.

## 5. CORRECTION TO THE ONE-PHOTON RECOMBINATION CROSS SECTION: TWO-LOOP APPROACH

In this part of the work we consider the case when the initial state  $a$  belongs to the continuous spectrum. Then, as noted above, an infinite number of resonances appear in expression (21), each of which requires regularization. The contributions from cascades, in terms of their magnitude, correspond to resonant one-photon transitions [28], which have already been accounted for in the kinetic equations of population balance in the calculation of the ionization degree of the primary hydrogen plasma [5, 6]. Earlier, various approaches were proposed to solve a similar problem arising for bound-bound transitions. In the work [30], resonant contributions to the two-photon amplitude (21) were discarded, and the remaining part was interpreted as the contribution from non-resonant («pure») radiation. However, as noted in [13, 18], this approach loses gauge invariance. Non-resonant contributions calculated in this manner in the «length» and «velocity» forms differ significantly. Later, an approach was proposed, based on partitioning contributions into «windows», similar to the one described above [34]. However, as pointed out in [28], interference between resonant and non-resonant contributions can reach the same order of magnitude as «pure» two-photon radiation. Thus, none of the approaches provides an unambiguous way to separate the cascade process from the total radiation.

In this regard, in the works [18–20] it was first suggested to consider not the differential cross section of the two-photon transition probability, but the imagi-

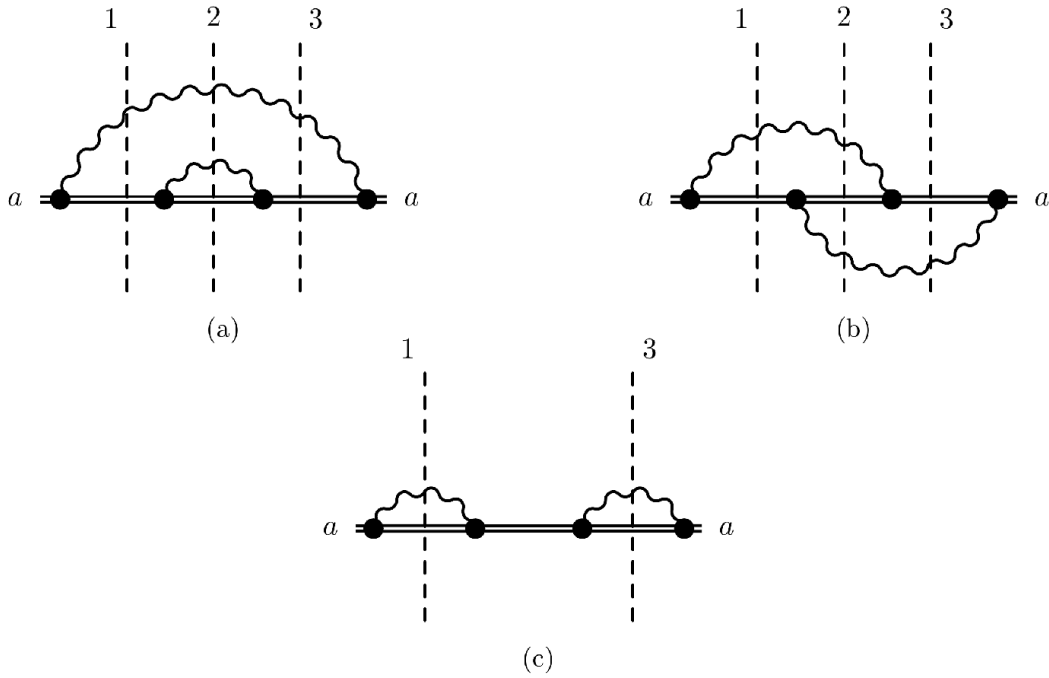


**Fig. 4.** Feynman diagrams for two-loop self-energy corrections for the bound electron in the state  $a$ : loop inside loop loops (a), crossed loops (b), and loop-after-loop contributions (c). The imaginary contributions from the poles of intermediate electron propagators, represented by «cuts» along the dashed vertical lines labeled 1 and 3, correspond to one-loop self-energy (SE) corrections to the one-photon process. Cuts along the dashed line labeled 2 correspond to the two-photon contribution,  $\Gamma_a^{(2\gamma)}$ , considered in this work. All notations are the same as in Fig. 1

nary part of the two-loop self-energy corrections. It was shown that for the state  $2s$  in the hydrogen atom, the quantity calculated in this manner coincides precisely with the transition rate of  $2s \rightarrow 1s + 2\gamma$  in the hydrogen atom, which is  $8.229 \text{ sec}^{-1}$  [44]. In addition, it was demonstrated that for the  $3s$  state, which can decay via two-photon processes through the intermediate resonant  $2p$  state, regularization of the imaginary part of the two-loop self-energy correction is unnecessary and the resulting quantity is gauge invariant. The authors [18–20] interpret this quantity as the probability of «pure» two-photon radiation. However, in [13, 45], it was shown that the calculated value of the imaginary part of the two-loop self-energy corrections within the «alternative approach» [18–20] can become negative. Thus, it does not represent a probability but rather a two-photon radiative correction to the one-photon width. Later, the same interpretation was given in the textbook [26].

Following the theory presented in [16], and the conclusions drawn in the previous sections of this work, as well as the discussion above, it can be expected that the two-photon radiative correction to the one-

photon recombination cross section can be obtained taking into account the imaginary part of the two-loop self-energy corrections. According to the «alternative approach», and computational methods outlined in works [18, 45], the two-photon radiative correction to the one-photon recombination cross section arises when considering two-loop self-energy diagrams for an electron from the continuum interacting with the Coulomb field of the nucleus. The second-order self-energy corrections, contributing to the two-photon correction to the atomic level width, are depicted in Fig. 4.

The Feynman diagrams in Figs. 4 a and 4 b are referred to as irreducible because they cannot be reduced to simpler ones by cutting only the internal electron line. In contrast, the imaginary part of the reducible «loop after loop» (LaL) diagram, Fig. 4 c, contributes solely to the one-loop self-energy correction to the one-photon recombination cross section and is not of further interest to us.

Within the S-matrix formalism the aforementioned «loop inside loop» (LiL, Fig. 4 a) and «crossed loops» (CL, Fig. 4 b) diagrams are given as follows:

$$\langle a|\widehat{S}^{(4)\text{LiL}}|a\rangle = (-ie)^4 \int d^4x_1 d^4x_2 d^4x_3 d^4x_4 \bar{\psi}_a(x_1) \gamma_{\mu_1} S(x_1, x_2) \gamma_{\mu_2} S(x_2, x_3) \times \gamma_{\mu_3} S(x_3, x_4) \gamma_{\mu_4} \psi_a(x_4) \times D_{\mu_1\mu_4}(x_1, x_4) D_{\mu_2\mu_3}(x_2, x_3), \tag{26}$$

and

$$\langle a'|\widehat{S}^{(4)\text{CL}}|a\rangle = (-ie)^4 \int d^4x_1 d^4x_2 d^4x_3 d^4x_4 \bar{\psi}_a(x_1) \gamma_{\mu_1} S(x_1, x_2) \gamma_{\mu_2} S(x_2, x_3) \times \gamma_{\mu_3} S(x_3, x_4) \gamma_{\mu_4} \psi_a(x_4) \times D_{\mu_1\mu_3}(x_1, x_3) D_{\mu_2\mu_4}(x_2, x_4), \tag{27}$$

respectively. Substituting the expressions (6) and (7) into (26), (27), and performing intermediate calculations, we obtain the loop-inside-loop contribution in the form

$$U_a^{(4)\text{LiL}} = e^4 \sum_{knm} \langle an|\frac{1-\alpha_1\alpha_4}{r_{14}} \frac{1-\alpha_2\alpha_3}{r_{23}} I_{nmka}^{\text{LiL}}(r_{14}, r_{23})|mk\rangle, \tag{28}$$

where

$$I_{nmka}^{\text{LiL}}(r_{14}, r_{23}) = \left(\frac{1}{2\pi i}\right)^2 \int_{-\infty}^{+\infty} d\omega_1 \int_{-\infty}^{+\infty} d\omega_3 \times \frac{e^{i|\omega_1|r_{14}} e^{i|\omega_3|r_{23}}}{(\mathcal{E}_a - \omega_1 - \mathcal{E}_n(1-i0))(\mathcal{E}_a - \omega_1 - \omega_3 - \mathcal{E}_k(1-i0))(\mathcal{E}_a - \omega_1 - \mathcal{E}_m(1-i0))}. \tag{29}$$

Similarly, for the crossed loops we find

$$U_a^{(4)\text{CL}} = e^4 \sum_k \langle an|\frac{1-\alpha_1\alpha_3}{r_{13}} \frac{1-\alpha_2\alpha_4}{r_{24}} I_{ka}^{\text{CL}}(r_{13}, r_{24})|mk\rangle, \tag{30}$$

along with the notation

$$I_{nmka}^{\text{CL}}(r_{13}, r_{24}) = \left(\frac{1}{2\pi i}\right)^2 \int_{-\infty}^{+\infty} d\omega_1 \int_{-\infty}^{+\infty} d\omega_3 \times \frac{e^{i|\omega_1|r_{13}} e^{i|\omega_3|r_{24}}}{(\mathcal{E}_a - \omega_1 - \mathcal{E}_n(1-i0))(\mathcal{E}_a - \omega_1 - \omega_3 - \mathcal{E}_k(1-i0))(\mathcal{E}_a - \omega_3 - \mathcal{E}_m(1-i0))}. \tag{31}$$

As mentioned above, radiative corrections to the probability of one-photon emission are related to the poles of the outer energy denominators in the expressions (29), (31), while the two-photon radiative correction is determined by the poles of the central energy denominator. For further calculations, we represent the integrals that contain factor  $e^{i|\omega|r}$  as follows:

$$\text{Re} \int_{-\infty}^{\infty} d\omega \frac{e^{i|\omega|r}}{\mathcal{E}_a - \mathcal{E}_k(1-i0) - \omega} = -\frac{\pi}{2} \left(1 + \frac{\mathcal{E}_k}{|\mathcal{E}_k|}\right) \left(1 + \frac{\beta_{ak}}{|\beta_{ak}|}\right) \sin(\beta_{ak}r), \tag{32}$$

where  $\beta_{ak} \equiv \mathcal{E}_a - \mathcal{E}_k$ . Performing integration over  $\omega$  using the expression (32), we find that the two-photon contributions of the expressions (29), (31) reduce to

$$I_{ka}^{\text{LiL}}(r_{14}, r_{23}) = \frac{e^4}{2\pi} \left(1 + \frac{\mathcal{E}_k}{|\mathcal{E}_k|}\right) \int_0^{\beta_{ak}} d\omega_1 \frac{\sin(\omega_1 r_{23}) e^{i(\beta_{ak}-\omega_1)r_{14}}}{(\mathcal{E}_a + \omega_1 - \mathcal{E}_n(1-i0))(\mathcal{E}_a - \omega_1 - \mathcal{E}_m(1-i0))},$$

and, respectively,

$$I_{ka}^{\text{CL}}(r_{13}, r_{24}) = \frac{e^4}{2\pi} \left(1 + \frac{\mathcal{E}_k}{|\mathcal{E}_k|}\right) \int_0^{\beta_{ak}} d\omega_1 \frac{\sin(\omega_1 r_{23}) e^{i(\beta_{ak}-\omega_1)r_{14}}}{(\mathcal{E}_a + \omega_1 - \mathcal{E}_n(1-i0))(\mathcal{E}_a - \omega_1 - \mathcal{E}_m(1-i0))}.$$

Combining the contributions and using the definition  $\Gamma_a^{(2\gamma)} = -2\text{Im} \Delta E_a^{21\text{SE}}$ , as well as introducing Feynman infinitesimal  $i0 \rightarrow i\eta$  parameters in the denominators, we obtain:

$$\Gamma_a^{(2\gamma)} = \sum_k \Gamma_{ak}^{(2\gamma)}, \quad (33)$$

where the partial widths  $\Gamma_{ak}^{(2\gamma)}$  is introduced as follows (see details in [13]):

$$\begin{aligned} \Gamma_{ak}^{(2\gamma)} = & e^4 \lim_{\eta \rightarrow 0} \text{Re} \int_0^{\beta_{ak}} d\omega \frac{\omega(\beta_{ak} - \omega)}{2^4 \pi^3} \int d\nu d\nu' \times \\ & \times \sum_{\lambda\lambda'} \sum_n \left\{ \frac{\langle k | \alpha \mathbf{A}_{k\lambda}^* | n \rangle \langle n | \alpha \mathbf{A}_{k'\lambda'}^* | a \rangle}{\mathcal{E}_a - \omega - \mathcal{E}_n(1 - i\eta)} + \frac{\langle k | \alpha \mathbf{A}_{k'\lambda'}^* | n \rangle \langle n | \alpha \mathbf{A}_{k\lambda}^* | a \rangle}{(\mathcal{E}_k - \mathcal{E}_n)(1 - i\eta) + \omega} \right\} \times \\ & \times \sum_m \left\{ \frac{(\langle k | \alpha \mathbf{A}_{k\lambda}^* | m \rangle)^* (\langle m | \alpha \mathbf{A}_{k'\lambda'}^* | a \rangle)^*}{\mathcal{E}_a - \omega - \mathcal{E}_m(1 - i\eta)} + \frac{(\langle k | \alpha \mathbf{A}_{k'\lambda'}^* | m \rangle)^* (\langle m | \alpha \mathbf{A}_{k\lambda}^* | a \rangle)^*}{(\mathcal{E}_k - \mathcal{E}_m)(1 - i\eta) + \omega} \right\}, \end{aligned} \quad (34)$$

where  $\nu \equiv \mathbf{k}/|\mathbf{k}|$  is the unit vector in the direction of the emitted photon.

The most important consequence of this approach («alternative approach» according to [18–20]) is the absence of the square of the amplitude modulus in the expression (34). As will be shown below, this fact allows us to perform the frequency integration  $\omega$  in (34) analytically and to avoid the divergent cascade contributions, see [13, 19]. According to the aforementioned works, the regularization procedure can be considered on these model integrals:

$$\lim_{\eta \rightarrow 0} \int_0^\infty d\omega \left| \frac{1}{A - \omega + i\eta} \right|^2 = \lim_{\eta \rightarrow 0} \frac{\pi + 2 \arctan(\frac{A}{\eta})}{2\eta}. \quad (35)$$

$$\lim_{\eta \rightarrow 0} \text{Re} \int_0^1 d\omega \left( \frac{1}{A - \omega + i\eta} \right)^2 = \frac{1}{A(A - 1)}, \quad (36)$$

where  $A$  is the positive real constant.

In contrast to Eq. (35), the real part of the squared amplitude in Eq. (36) is not divergent. The result (36) holds only under the following conditions: 1) the infinitesimal parameters  $i\eta$  must be preserved in both energy denominators of the expression (36) and set equal to each other. 2) in the expression (36), the integration over the frequency  $\omega$  is first performed, and only then the limit  $\eta \rightarrow 0$  is taken. Both of these conditions correspond to the formulation of the Gellman-Low-Sucher theorem for calculating radiative corrections to energy levels [46, 47]. Thus, the regularization in Eq. (36) arises naturally when calculating the imaginary part of the two-loop level shift.

Let us now turn to the non-relativistic limit of the expression (34). After integrating over the directions of the emitted photons and summing over the polarizations, we obtain the final expression for the two-photon radiative correction to the partial one-photon transition  $a \rightarrow a'$ :

$$\begin{aligned} \Gamma_{aa'}^{(2\gamma)} = & \frac{4e^4}{9\pi} \frac{1}{2l_a + 1} \lim_{\eta \rightarrow 0} \text{Re} \sum_{m_a m_{a'}} \int_0^{\omega_{aa'}} d\omega \omega^3 (\omega_{aa'} - \omega)^3 \times \\ & \times \sum_{nn'} \left( \frac{\langle a' | \mathbf{r} | n \rangle \langle n | \mathbf{r} | a \rangle}{E_n - E_a + \omega + i\eta} + \frac{\langle a' | \mathbf{r} | n \rangle \langle n | \mathbf{r} | a \rangle}{E_n - E_{a'} - \omega + i\eta} \right) \times \\ & \times \left( \frac{\langle a' | \mathbf{r} | n' \rangle^* \langle n' | \mathbf{r} | a \rangle^*}{E_{n'} - E_a + \omega + i\eta} + \frac{\langle a' | \mathbf{r} | n' \rangle^* \langle n' | \mathbf{r} | a \rangle^*}{E_{n'} - E_{a'} - \omega + i\eta} \right). \end{aligned} \quad (37)$$

where the matrix elements in the numerators are assumed to be taken with the Schrödinger wave functions. For the case when  $a$  and  $a'$  are the bound states, the partial two-photon corrections were evaluated in [13, 18]. The equation (37) differs from Eq. (23) with respect to the formulation of the model integrals, as specified in Eqs. (35), (36).

The finite-temperature generalization, which accounts for induced processes, with two thermal loops, can be found in [45]. Unlike the bound-bound transitions, a distinct scenario emerges when the initial state  $a$  belongs the continuum spectrum, i.e.,  $a = \varepsilon$ . An infinite number of resonances requires regularization as described in Eq. (36). To define the two-photon cor-

**Table 1.** The one-photon spontaneous recombination coefficients  $\alpha_{nl}^{(1\gamma)}$  for  $1s$ ,  $2s$  and  $3s$  states of hydrogen at different electron temperatures  $T$  (in Kelvin). All the values are expressed in units of  $\text{m}^3\text{s}^{-1}$

$T$	77	300	1000	3000	5000	$10^4$
$1s$	$1.876 \cdot 10^{-18}$	$9.494 \cdot 10^{-19}$	$5.185 \cdot 10^{-19}$	$2.969 \cdot 10^{-19}$	$2.281 \cdot 10^{-19}$	$1.582 \cdot 10^{-19}$
$2s$	$2.749 \cdot 10^{-19}$	$1.392 \cdot 10^{-19}$	$7.612 \cdot 10^{-20}$	$4.372 \cdot 10^{-20}$	$3.366 \cdot 10^{-20}$	$2.342 \cdot 10^{-20}$
$3s$	$9.251 \cdot 10^{-20}$	$4.685 \cdot 10^{-20}$	$2.562 \cdot 10^{-20}$	$1.469 \cdot 10^{-20}$	$1.129 \cdot 10^{-20}$	$7.816 \cdot 10^{-21}$
$4s$	$4.335 \cdot 10^{-20}$	$2.194 \cdot 10^{-20}$	$1.198 \cdot 10^{-20}$	$6.835 \cdot 10^{-21}$	$5.230 \cdot 10^{-21}$	$3.587 \cdot 10^{-21}$

rection to the one-photon recombination cross section  $\sigma_{a'}^{(1\gamma)}$ , we employ the relation:

$$\sigma_{a'}^{(2\gamma)} = \frac{\Gamma_{a'\varepsilon}^{(2\gamma)}}{j}. \quad (38)$$

### 6. DETAILS OF NUMERICAL CALCULATIONS

The main problem in the numerical evaluation of equations (33) and (37) lies in the summation over the spectrum of intermediate and final states. In this work, we addressed this challenge by solving the Schrödinger equation numerically using the B-spline method [40, 41, 48]. This approach enables efficient computation of sum over the states. The B-spline method is well-established in relativistic atomic theory and has proven effective for both fully relativistic calculations of various quantum electrodynamics (QED) corrections and non-relativistic approximations of complex expressions involving multiple sums. Using the explicit form of the initial state wave function of continuum spectrum, we generated the corresponding radial matrix elements and atomic quasi-energies. Imposing the condition of dual kinetic balance [48] prevents the emergence of spurious states. Thus, replacing the «real» spectrum with a quasi-complete one leads to rapid convergence of the calculated sums. In our computations, we utilize ninth-order B-splines with atomic spectrum of forty states.

In studies of radiation transfer, the most important physical quantity is the recombination coefficient,  $\alpha_{nl}^{(1\gamma)}$ . For the atomic level with principal quantum number  $n$  and orbital angular momentum  $l$  it is defined as

$$\alpha_{nl}^{(1\gamma)} = \int_0^\infty \sigma_{nl}^{(1\gamma)}(v) f(v) v dv, \quad (39)$$

where the cross section  $\sigma_{nl}^{(1\gamma)}(v)$  is given by Eq. (16). The Maxwell–Boltzmann distribution,  $f(v)$ , with  $v = p$  in atomic units, is

$$f(v)dv = 4\pi \left( \frac{1}{2\pi k_B T} \right)^{3/2} v^2 e^{-\frac{v^2}{2k_B T}} dv. \quad (40)$$

Here  $k_B$  is the Boltzmann constant,  $T$  is the electron temperature in Kelvin. Correction  $\alpha_{nl}^{(2\gamma)}$  can be calculated in a similar way by replacing  $\sigma_{nl}^{(1\gamma)}(v) \rightarrow \sigma_{nl}^{(2\gamma)}(v)$  in Eq. (39), in conjunction with expressions (37), (38).

The integration over frequency and velocity in Eqs. (37) and (39) was performed numerically. The resulting one-photon recombination coefficients,  $\alpha_{nl}^{(1\gamma)}$  (see Eq. (39)), are collected in Tab. 1 in a wide range of electron temperatures for several lower states of the hydrogen atom.

The values obtained for  $\alpha_{nl}^{(1\gamma)}$  show excellent agreement with those reported in [16, 49].

The results of calculations of the two-photon correction to the one-photon recombination coefficient are presented in Tab. 2 (see also Fig. 5) for the same states and temperatures. The values for the two-photon correction  $\alpha_{nl}^{(2\gamma), \text{ind}}$  stimulated by the blackbody radiation environment is present in Tab. 3 (see also Fig. 6). The latter can be obtained from Eqs. (37) and (38) by substitution of the additional multiplier  $(1 + n_\beta(\omega))(1 + n_\beta(\omega_{aa'} - \omega))$  into the integral over frequency, see, e.g., [35]. Here,  $n_\beta(\omega) = [\exp(\beta\omega) - 1]^{-1}$  denotes the Bose–Einstein distribution function, and  $\beta = 1/(k_B T)$ , where  $k_B$  is the Boltzmann constant and  $T$  is the temperature in kelvins. Then the first contribution, represented by a unit, corresponds to the two-photon correction for the spontaneous process, while the additional contributions (depending on  $n_\beta$ ) are the stimulated ones.

It should be emphasized that the appearance of negative values for  $\alpha_{nl}^{(2\gamma), \text{ind}}$  should not cause significant difficulties. The fact is that the coefficients  $\alpha_{nl}^{(2\gamma)}$  as well as  $\alpha_{nl}^{(2\gamma), \text{ind}}$  are the result of calculating the imaginary part of the two-loop self-energy. The latter represents a radiative QED correction to the one-photon recombination process. Thus, the quantities  $\alpha_{nl}^{(2\gamma)}$ ,  $\alpha_{nl}^{(2\gamma), \text{ind}}$  are radiative corrections to the recombination coefficients  $\alpha_{nl}^{(1\gamma)}$ . Since such contributions may assume neg-

**Table 2.** The two-photon correction  $\alpha_{nl}^{(2\gamma)}$  to one-photon spontaneous recombination coefficients for  $1s$ ,  $2s$  and  $3s$  states of hydrogen at different electron temperatures  $T$  (in Kelvin). All the values are expressed in units of  $\text{m}^3\text{s}^{-1}$

$T$	77	300	1000	3000	5000	$10^4$
$1s$	$4.554 \cdot 10^{-23}$	$1.969 \cdot 10^{-23}$	$6.468 \cdot 10^{-24}$	$1.666 \cdot 10^{-24}$	$8.204 \cdot 10^{-25}$	$3.024 \cdot 10^{-25}$
$2s$	$4.217 \cdot 10^{-25}$	$2.081 \cdot 10^{-25}$	$7.511 \cdot 10^{-26}$	$2.001 \cdot 10^{-26}$	$9.889 \cdot 10^{-27}$	$3.651 \cdot 10^{-27}$
$3s$	$4.061 \cdot 10^{-26}$	$2.365 \cdot 10^{-26}$	$1.011 \cdot 10^{-26}$	$2.939 \cdot 10^{-27}$	$3.651 \cdot 10^{-27}$	$5.453 \cdot 10^{-28}$
$4s$	$6.220 \cdot 10^{-27}$	$3.801 \cdot 10^{-27}$	$1.735 \cdot 10^{-27}$	$4.987 \cdot 10^{-28}$	$2.527 \cdot 10^{-28}$	$9.549 \cdot 10^{-29}$

**Table 3.** The two-photon correction  $\alpha_{nl}^{(2\gamma)\text{ind}}$  to one-photon recombination coefficients induced by BBR field for  $1s$ ,  $2s$  and  $3s$  states of hydrogen at different electron temperatures  $T$  (in Kelvin). All the values are expressed in units of  $\text{m}^3\text{s}^{-1}$

$T$	77	300	1000	3000	5000	$10^4$
$1s$	$9.066 \cdot 10^{-30}$	$2.167 \cdot 10^{-28}$	$2.339 \cdot 10^{-27}$	$2.235 \cdot 10^{-26}$	$3.332 \cdot 10^{-26}$	$4.373 \cdot 10^{-26}$
$2s$	$7.125 \cdot 10^{-31}$	$1.822 \cdot 10^{-29}$	$1.908 \cdot 10^{-28}$	$2.476 \cdot 10^{-27}$	$3.570 \cdot 10^{-27}$	$4.385 \cdot 10^{-27}$
$3s$	$2.133 \cdot 10^{-31}$	$9.648 \cdot 10^{-31}$	$-1.548 \cdot 10^{-29}$	$4.671 \cdot 10^{-28}$	$7.895 \cdot 10^{-28}$	$1.147 \cdot 10^{-27}$
$4s$	$1.350 \cdot 10^{-37}$	$-2.026 \cdot 10^{-35}$	$-2.069 \cdot 10^{-32}$	$2.503 \cdot 10^{-30}$	$1.566 \cdot 10^{-29}$	$4.995 \cdot 10^{-28}$

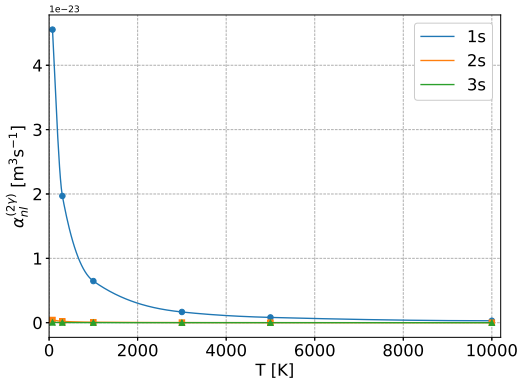


**Fig. 5.** Temperature dependence of the two-photon radiative correction  $\alpha_{nl}^{2\gamma}$  [ $\text{m}^3\text{s}^{-1}$ ] associated with spontaneous recombination

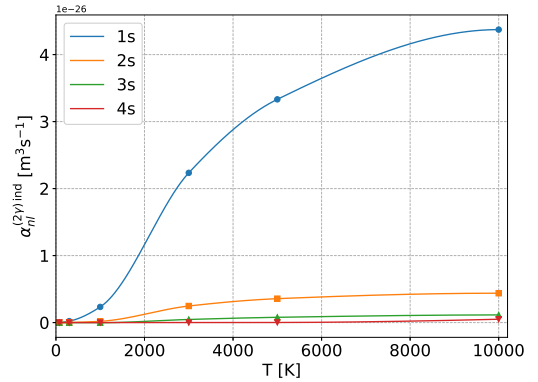


**Fig. 6.** Temperature dependence of the stimulated part of two-photon radiative correction  $\alpha_{nl}^{2\gamma,\text{ind}}$  [ $\text{m}^3\text{s}^{-1}$ ] associated with induced recombination.

ative values, they cannot be interpreted as two-photon widths or as a genuine two-photon recombination process; see [13, 15]. This correction slightly diminishes the dominant one-photon term but does not affect the positive overall value of the recombination coefficient.

Using the values for the two-photon correction given in Tab. 2 and Tab. 3, the following fit for

$$\alpha_{nl}^{\text{total}}(T) = 10^{-19} a \left( \sum_{k=1}^3 t^k \right)^b \exp(-ct^d) [\text{m}^3 \cdot \text{s}^{-1}], \quad (41)$$

where the coefficients  $a$ ,  $b$ ,  $c$ , and  $d$  are summarized in Tab. 4 and  $t = T/1000$ . The correction computed and fitted in this way can be easily incorporated into any-type of modern recombination codes [50].

The impact of the two-photon correction  $\alpha_{nl}^{(2\gamma)}$  on the recombination kinetics of hydrogen plasma within the three-level approximation is discussed in the next section.

**Table 4.** Parameters of the fit given by Eq. (41)

$nl$	$a$	$b$	$c$	$d$
$1s$	0.1440	0.6572	8.420	0.2785
$2s$	0.003403	0.8842	9.358	0.2859
$3s$	$2.530 \cdot 10^{-7}$	-0.2979	0.4911	0.2453
$4s$	$5.428 \cdot 10^{-8}$	-0.1799	0.9089	0.4265

### 7. APPLICATION TO THE COSMOLOGICAL RECOMBINATION PROBLEM

An important characteristics of the cosmological recombination at the given redshift is the ionization fraction,  $x_e$ , of the primordial plasma. This quantity determines the ratio of free electron density to the total density of hydrogen atoms and ions. Ionization fraction is defined by the set of kinetic balance equations for the level populations which accounts for all possible radiative decay channels to the ground state. Within the 3-level approximation (ground state, first excited state, and continuum), this system can be reduced to one ordinary differential equation [6]. The standard three-level recombination model incorporates only the two channels through which the atom can transition directly to the ground state (i.e. to finally recombine): Ly $_{\alpha}$  transition  $2p \rightarrow 1s + \gamma(E1)$  and two-photon decay  $2s \rightarrow 1s + 2\gamma(E1)$ .

To estimate the contribution  $\alpha_{nl}^{(2\gamma)}$  to the ionization history, we start from the differential equation for the ionization fraction  $x_e = n_e/n_H$ , where  $n_e$  is the number density of free electrons and  $n_H$  is the total number density of hydrogen atoms and ions. The latter depend on redshift  $z$  as

$$n_H = n_H^0(1+z)^3, \quad (42)$$

where  $n_H^0$  is the value of the hydrogen concentration in the present epoch. The radiation temperature dependence on redshift  $z$  is given by

$$T = T_0(1+z), \quad (43)$$

where  $T_0 = 2.725$  K is the present temperature of CMB radiation.

The time-dependent behavior of the hydrogen ionization fraction in the expanding isotropic homogeneous universe within the 3-level model of the atom [3, 5, 6] is described by the kinetic equation:

$$\frac{dx_e}{dz} = C_H \frac{\left[ \alpha_H x_e^2 n_H - \beta_H \exp\left(-\frac{\Delta E_{21}}{k_B T}\right) (1 - x_e) \right]}{H(z)(1+z)}, \quad (44)$$

$$C_H = \frac{1 + K_H W_{2s,1s}^{(2\gamma)} n_H (1 - x_e)}{1 + K_H \left( W_{2s,1s}^{(2\gamma)} + \beta_H \right) n_H (1 - x_e)}, \quad (45)$$

$$K_H = \frac{\lambda_{\alpha}^3}{8\pi H(z)}. \quad (46)$$

Here  $\alpha_H$  is the total Case B recombination coefficient,  $\alpha_H \equiv \sum_{nl \geq 2s} \alpha_{nl}^{(1\gamma)}$ ,  $\beta_H$  is the total ionization

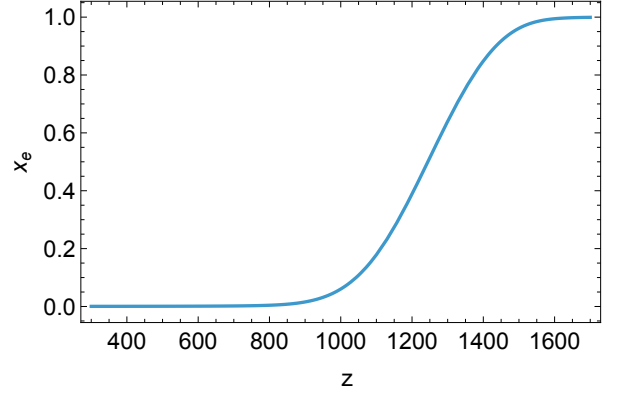


Fig. 7. Ionization fraction  $x_e$  as a function of redshift  $z$

coefficient,  $\lambda_{\alpha}$  is the wavelength of Ly $_{\alpha}$  transition,  $W_{2s,1s}^{(2\gamma)} = 8.229 \text{ s}^{-1}$  is the transition rate of spontaneous two-photon emission,  $\Delta E_{21} = E_{2s} - E_{1s}$  and  $H(z)$  is the Hubble factor describing the expansion of universe within the considered cosmological model.

Typically, for the three-level models, the Case B recombination coefficient is fitted as follows [5]:

$$\alpha_H = 10^{-19} \frac{at^b}{1 + ct^d} [\text{m}^3 \text{ s}^{-1}], \quad (47)$$

with  $t = T/10^4$  K,  $a = 4.309$ ,  $b = -0.6166$ ,  $c = 0.6703$  and  $d = 0.5300$ .

Then according to the Milne relation the ionization coefficient  $\beta_H$  can be expressed in terms of recombination coefficient [6]:

$$\beta_H(z) = \alpha_H(z) g(z) \exp\left(-\frac{E_{2s}}{k_B T(z)}\right), \quad (48)$$

where

$$g(z) = \left( \frac{2\pi m_e k_B T(z)}{h^2} \right)^{3/2}. \quad (49)$$

Substituting all parameters of the recombination model (see, in particular, [5, 6]) into Eq. (44), its numerical solution yields the dependence of the ionization fraction on redshift, as illustrated in Fig. 7.

In order to incorporate the two-photon correction to the one-photon recombination coefficients, the coefficient  $\alpha_H$  should be expressed in the following form:

$$\alpha_H \equiv \sum_{nl \geq 2s} \alpha_{nl}^{(1\gamma)} + \sum_{nl \geq 2s} \alpha_{nl}^{(2\gamma)}, \quad (50)$$

where the first term corresponds to Eq. (47), and the second term can be represented as a sum of fit given by Eq. (41). From Tab. 2 it follows that the values of  $\alpha_{nl}^{(2\gamma)}$  decrease with increasing principal quantum number  $n$ . At the temperatures of the recombination epoch,

$1000 \leq T \leq 5000$  K, the relative contribution of  $\alpha_{nl}^{(2\gamma)}$  is of the order of  $10^{-5}$ – $10^{-6}$  for the  $2s$  state. Therefore, one can expect the resulting modification in the ionization fraction,  $\Delta x_e/x_e$ , is likewise about  $10^{-5}$ – $10^{-6}$ .

Such contribution is about of two orders of magnitude below the current experimental accuracy, which requires theoretical models to achieve a precision at the level of 0.1% [2]. However, over the past two decades, numerous effects that influence the ionization fraction have been discussed in the literature. Of particular interest are the dark matter annihilation, the effect of multipole transitions and higher excited states [51]. The magnitude of these effects is comparable to the two-photon correction to the one-photon recombination coefficient considered here. Modern multilevel theoretical models used to compute the ionization history account for all relevant effects down to the level of  $10^{-5}$ – $10^{-6}$ . Therefore, the correction  $\alpha_{nl}^{(2\gamma)}$ , although small, becomes significant in the context of high-precision cosmology. It must be included in any model aiming to match the sensitivity of current and future cosmological observations, such as those from the Planck satellite or the upcoming CMB-S4 experiment [52].

## 8. CONCLUSION

In this work, using the hydrogen atom as a benchmark system, the two-loop self-energy corrections to the one-photon recombination cross section were investigated within the framework of relativistic quantum electrodynamics. An explicit analytical expression for the two-photon contribution of the two-loop self-energy correction to the one-photon recombination coefficient was derived. Notably, it has been shown that this expression is free of singularities, unlike the two-photon recombination cross section, which typically includes divergent resonant contributions from cascade transitions.

To explore the physical implications of the found radiative correction to one-photon recombination rate, we performed numerical computations by convolving the corrected one-photon cross section with a Maxwell distribution for free electrons. These calculations cover recombination into the  $1s$ ,  $2s$  and  $3s$  bound states across a wide range of electron temperatures  $T$ . To clarify the temperature dependence and magnitude of the correction  $\alpha_{nl}^{(2\gamma)}$ , numerical results are presented in Figs. 5, 6. The constructed dependencies for several lower states provide valuable information about the role of the two-photon correction to the one-photon recom-

ination cross section under thermodynamic conditions of cosmological and laboratory plasma.

We further incorporated calculated corrections into a simplified three-level model of hydrogen recombination in the early Universe. The resulting impact on the ionization fraction, while modest, approaches the numerical precision of current state-of-the-art theoretical models [10,50]. Although this correction remains below the threshold of present observational sensitivity [53], it underscores the importance of including higher-order QED effects in precision cosmology and highlights the need for more advanced observational techniques (see, for example, Fig. 3.5 in [54]).

**Acknowledgements.** The work was carried out with the support of grants from the Foundation for the Advancement of Theoretical Physics and Mathematics BASIS grants № 23-1-3-31-1 and № 25-1-2-18-1. E. S. would like to thank Saint-Petersburg State University for the financial support within the project № 122040800256-8.

## REFERENCES

1. G. P. Lynch, L. Knox, and J. Chluba, *Desi Observations and the Hubble Tension in Light of Modified Recombination*, Physical Review D **110**, 083513, (2024).
2. Y. Kulinich and B. Novosyadlyj, *Distortion of the CMB Spectrum by the First Molecules of the Dark Ages*, Astronomy and Astrophysics **698**, A32, (2025).
3. P. J. E. Peebles, *Recombination of the Primeval Plasma*, The Astrophysical Journal **153**, 1, (1968).
4. Y. B. Zeldovich, V. G. Kurt, and R. A. Syunyaev, *Recombination of Hydrogen in the Hot Model of the Universe*, Zhurnal Eksperimentalnoi i Teoreticheskoi Fiziki **55**, 278, (1968).
5. S. Seager, D. D. Sasselov, and D. Scott, *A New Calculation of the Recombination Epoch*, The Astrophysical Journal **523**, L1, (1999).
6. S. Seager, D. D. Sasselov, and D. Scott, *How Exactly Did the Universe Become Neutral?*, The Astrophysical Journal Supplement Series **128**, 407, (2000).
7. J. Chluba, *Could the Cosmological Recombination Spectrum Help Us Understand Annihilating Dark Matter?*, Monthly Notices of the Royal Astronomical Society **402**, 1195, (2010).
8. L. Hart and J. Chluba, *Using the Cosmological Recombination Radiation to Probe Early Dark Energy and Fundamental Constant Variations*, Monthly Notices of the Royal Astronomical Society **519**, 3664, (2022).

9. N. Lee and Y. Ali-Haïmoud, *Hyrec-2: A Highly Accurate Sub-millisecond Recombination Code*, Physical Review D **102**, 083518, (2020).
10. H. Liu, G. W. Ridgway, and T. R. Slatyer, *Code Package for Calculating Modified Cosmic Ionization and Thermal Histories with Dark Matter and Other Exotic Energy Injections*, Physical Review D **101**, 023504, (2020).
11. Y. Ali-Haimoud and C. M. Hirata, *Hyrec: A Fast and Highly Accurate Primordial Hydrogen and Helium Recombination Code*, Physical Review D **83**, 023505, (2011).
12. L. Pogosian, G.-B. Zhao, and K. Jedamzik, *A Consistency Test of the Cosmological Model at the Epoch of Recombination Using DESI Baryonic Acoustic Oscillation and Planck Measurements*, The Astrophysical Journal Letters **973**, L13, (2024).
13. T. Zalialiutdinov, D. Solovyev, L. Labzowsky, *et al.*, *Two-photon Transitions with Cascades: Two-photon Transition Rates and Two-photon Level Widths*, Phys. Rev. A **89**, 052502, (2014).
14. D. Solovyev and E. Solovyeva, *Rydberg-state Mixing in the Presence of an External Electric Field: Comparison of the Hydrogen and Antihydrogen Spectra*, Phys. Rev. A **91**, 042506, (2015).
15. T. A. Zalialiutdinov, D. A. Solovyev, L. N. Labzowsky, *et al.*, *QED Theory of Multiphoton Transitions in Atoms and Ions*, Phys. Rep. **737**, 1, (2018).
16. D. Solovyev, T. Zalialiutdinov, A. Anikin, *et al.*, *Recombination Process for the Hydrogen Atom in the Presence of Blackbody Radiation*, Phys. Rev. A **100**, 012506, (2019).
17. T. Zalialiutdinov, A. Anikin, and D. Solovyev, *Two-photon Atomic Level Widths at Finite Temperatures*, Physical Review A **102**, 032204, (2020).
18. U. D. Jentschura, *Non-uniform Convergence of Two-photon Decay Rates for Excited Atomic States*, Journal of Physics A: Mathematical and Theoretical **40**, F223, (2007).
19. U. D. Jentschura, *Two-photon Decays Reexamined: Cascade Contributions and Gauge Invariance*, Journal of Physics A: Mathematical and Theoretical **41**, 155307, (2008).
20. U. D. Jentschura and A. Surzhykov, *Relativistic Calculation of the Two-photon Decay Rate of Highly Excited Ionic States*, Physical Review A **77**, 042506, (2008).
21. O. Y. Andreev, L. N. Labzowsky, G. Plunien, *et al.*, *QED Theory of the Spectral Line Profile and Its Applications to Atoms and Ions*, Phys. Rep. **455**, 135, (2008).
22. L. D. Landau and E. M. Lifshitz, *Quantum Mechanics: Non-Relativistic Theory*. Pergamon Press, (1965).
23. V. Shabaev, *Two-time Green's Function Method in Quantum Electrodynamics of High-Z Few-electron Atoms*, Physics Reports **356**, 119, (2002).
24. U. D. Jentschura, *Self-energy Correction to the Two-photon Decay Width in Hydrogenlike Atoms*, Phys. Rev. A **69**, 052118, (2004).
25. L. Labzowsky, G. Klimchitskaya, and Y. Dmitriev, *Relativistic Effects in the Spectra of Atomic Systems*. Institute of Physics Publishing, (1993).
26. U. D. Jentschura and G. S. Adkins, *Quantum Electrodynamics: Atoms, Lasers and Gravity*. World Scientific, (2021).
27. A. I. Akhiezer and V. B. Berestetskii, *Quantum Electrodynamics*. Wiley-Interscience, New York, (1965).
28. L. Labzowsky, D. Solovyev, and G. Plunien, *Two-photon Decay of Excited Levels in Hydrogen: The Ambiguity of the Separation of Cascades and Pure Two-photon Emission*, Phys. Rev. A **80**, 062514, (2009).
29. L. N. Labzowsky and A. V. Shonin, *QED Theory of Cascades and Two-photon Transitions and Calculation of the E1–M1 Transition Probability in Two-electron Highly Charged Ions*, Phys. Rev. A **69**, 012503, (2004).
30. J. Chluba and R. A. Sunyaev, *Two-photon Transitions in Hydrogen and Cosmological Recombination*, Astronomy and Astrophysics **480**, 629, (2008).
31. J. Chluba and R. A. Sunyaev, *Ly-alpha Escape During Cosmological Hydrogen Recombination: The 3d-1s and 3s-1s Two-photon Processes*, A&A **512**, A53, (2010).
32. J. Chluba and R. A. Sunyaev, *Induced Two-photon Decay of the 2s Level and the Rate of Cosmological Hydrogen Recombination*, A&A **446**, 39, (2006).
33. C. M. Hirata and E. R. Switzer, *Primordial Helium Recombination. II. Two-photon Processes*, Phys. Rev. D **77**, 083007, (2008).
34. C. M. Hirata and E. R. Switzer, *Primordial Helium Recombination. II. Two-photon Processes*, Phys. Rev. D **77**, 083007, (2008).

35. E. E. Kholupenko and A. V. Ivanchik, *Two-photon  $2s - 1s$  Transitions During Hydrogen Recombination in the Universe*, *Ast. Lett.* **32**, 795, (2006).
36. P. Amaro, J. P. Santos, F. Parente, A. Surzhykov, and P. Indelicato, *Resonance Effects on the Two-photon Emission from Hydrogenic Ions*, *Phys. Rev. A* **79**, 062504, (2009).
37. N. L. Manakov, L. P. Rapoport, and S. A. Zapryagaev, *Relativistic Electromagnetic Susceptibilities of Hydrogen-like Atoms*, *Journal of Physics B: Atomic and Molecular Physics* **7**, 1076, (1974).
38. N. Manakov, V. Ovsianikov, and L. Rapoport, *Atoms in a Laser Field*, *Physics Reports* **141**, 320, (1986).
39. L. Labzowsky and D. Solovyev, *Coulomb Green Function and Its Applications in Atomic Theory*, pp. 15–34. Springer Berlin Heidelberg, (2003).
40. W. R. Johnson, S. A. Blundell, and J. Sapirstein, *Finite Basis Sets for the Dirac Equation Constructed from B Splines*, *Phys. Rev. A* **37**, 307, (1988).
41. J. Sapirstein and W. R. Johnson, *The Use of Basis Splines in Theoretical Atomic Physics*, *J. Phys. B* **29**, 5213, (1996).
42. F. Low, *Natural Line Shape*, *Phys. Rev.* **88**, 53, (1952).
43. T. A. Zalyalyutdinov, D. A. Solovyev, and L. N. Labzovskii,  *$4s-1s$  Two-photon Decay in Hydrogen Atom with Allowance for Cascades*, *Optics and Spectroscopy* **110**, 328, (2011).
44. L. N. Labzowsky, A. V. Shonin, and D. A. Solovyev, *QED Calculation of  $E1-M1$  and  $E1-E2$  Transition Probabilities in One-electron Ions with Arbitrary Nuclear Charge*, *J. Phys. B: At. Mol. and Opt. Phys.* **38**, 265, (2005).
45. T. Zaliutdinov, A. Anikin, and D. Solovyev, *Two-photon Atomic Level Widths at Finite Temperatures*, *Phys. Rev. A* **102**, 032204, (2020).
46. M. Gell-Mann and F. Low, *Bound States in Quantum Field Theory*, *Phys. Rev.* **84**, 350, (1951).
47. J. Sucher, *S-matrix Formalism for Level-shift Calculations*, *Phys. Rev.* **107**, 1448, (1957).
48. V. M. Shabaev, I. I. Tupitsyn, V. A. Yerokhin, G. Plumien, and G. Soff, *Dual Kinetic Balance Approach to Basis-set Expansions for the Dirac Equation*, *Physical Review Letters* **93**, 130401, (2004).
49. W. J. Boardman, *The Radiative Recombination Coefficients of the Hydrogen Atom*, *The Astrophysical Journal Supplement Series* **9**, 185, (1964).
50. J. Chluba and Y. Ali-Ha?moud, *Cosmospec: Fast and Detailed Computation of the Cosmological Recombination Radiation from Hydrogen and Helium*, *Monthly Notices of the Royal Astronomical Society* **456**, 3494, (2016).
51. D. Grin and C. M. Hirata, *Cosmological Hydrogen Recombination: The Effect of Extremely High- $n$  States*, *Phys. Rev. D* **81**, 083005, (2010).
52. R. W. Besuner, *Design, Planning, and Performance of the CMB- $S_4$  Experiment*, in *Ground-based and Airborne Telescopes IX* (H. K. Marshall, J. Spyromilio, and T. Usuda, eds.), p. 46, SPIE, (2022).
53. D. L. Clements, *An Introduction to the Planck Mission*, *Contemporary Physics* **58**, 331, (2017).
54. Y. Ali-Haimoud, *A New Spin on Primordial Hydrogen Recombination and a Refined Model for Spinning Dust Radiation*. PhD thesis, California Institute of Technology, (2011).